Virus Research 264 (2019) 32–39

Contents lists available at ScienceDirect

Virus Research

journal homepage: www.elsevier.com/locate/virusres

Interplay between CTHRC1 and the SU protein of avian leukosis virus subgroup J (ALV-J) facilitates viral replication

Yu Pang[a], Defang Zhou[a], Jingwen Xue[a], Jing Zhou[a], Ya Zhang[a], Gaoying Zheng[a], Shiyu Yuan[a], Yongxiu Yao[b], Ziqiang Cheng[a,*]

[a] College of Veterinary Medicine, Shandong Agricultural University, Tai'an, China
[b] The Pirbright Institute & UK-China Centre of Excellence on Avian Disease Research, Pirbright, Ash Road, Guildford, Surrey, GU24 0NF, UK

ARTICLE INFO

Keywords:
ALV-J
Proteomics
CTHRC1
Viral replication

ABSTRACT

The lifecycle of avian leukosis virus subgroup J (ALV-J), a typical tumorigenic retrovirus, is highly dependent upon host cellular proteins. However, there have been few studies directed at uncovering the host proteins responsible for ALV-J replication, which could provide insights into new strategies for ALV-J prevention and control. Here, we used proteomics to identify the association of differential levels of collagen triple helix-repeat-containing 1 (CTHRC1) and with viral replication. Our results revealed that CTHRC1 was significantly upregulated in ALV-J-infected cells *in vitro*, and these findings were confirmed *in vivo*. Additionally, *CTHRC1* overexpression facilitated ALV-J replication, whereas *CTHRC1* knockdown suppressed this activity. Moreover, we found that ALV-J drove CTHRC1 translocation from the nucleus to the cytosol through interactions with the ALV-J envelope glycoprotein. These results revealed CTHRC1 as a shutting protein is recruited by ALV-J to facilitate viral replication.

1. Introduction

Avian leukosis viruses (ALVs) are classified into 10 subgroups (A–J) that cause great economic losses in the poultry industry worldwide (Feng et al., 2016). In particular, more attention has been paid to the J subgroup of ALV (ALV-J) since isolation of the first strain (HPRS-103) from meat-type chickens in the United Kingdom in 1988. Subsequently, the virus was detected in China in 1999, with the strain eventually identified as having a wider neoplastic spectrum (Payne et al., 1991; Payne and Nair, 2012). ALV-J infection is closely related to the onset of visceral and vascular neoplasms with associated adverse consequences, including stunted growth, decreased egg production, and increased mortality (Li et al., 2017; Lin et al., 2016; Peng et al., 2015; Wang et al., 2018). ALV-J is considered to have emerged through a recombination event between an unknown exogenous ALV and an endogenous retrovirus (Payne et al., 1991; Smith et al., 1999) and was initially found to mainly infect meat chickens; however, subsequent studies found that ALV-J could also infect layer hens and local breeds (Cheng et al., 2005; Sun and Cui, 2007).

Similar to other retroviruses, ALV-J requires reverse-transcriptase-mediated transformation of the viral genome from RNA to proviral DNA and its integration into the host genome during replication. Subsequently, viral RNA is generated by the transcription of proviral DNA and further translated to produce various precursor and mature proteins that constitute virions (Lesbats and Parissi, 2018). ALV-J replication is complex and tightly regulated; however, the cellular proteins required for ALV-J replication remain unclear.

Collagen triple helix-repeat-containing 1 (CTHRC1) is a ~25-kDa secreted extracellular-matrix glycoprotein harboring a C-terminal globular domain, a short collagen triple-helix repeat of 36 amino acids, and an N-terminal signaling peptide for extracellular secretion (Ma et al., 2014; Wang and Fang, 2010). CTHRC1 was initially found in

Abbreviations: ALV-J, avian leukosis virus subgroup J; CLSM, confocal laser scanning microscopy; Co-IP, co-immunoprecipitation; CTHRC1, collagen triple helix-repeat-containing 1; DAPI, 4′6-diamidino-2-phenylindole; DMEM, Dulbecco's modified Eagle medium; ELISA, enzyme-linked immunosorbent assay; FITC, fluorescein isothiocyanate; GO, Gene Ontology; PBS, phosphate-buffered saline; PMSF, phenylmethylsulfonyl fluoride; RIPA, radioimmunoprecipitation assay; RNAi, RNA interference; shNC, control short-hairpin RNA; shRNA, short-hairpin RNA; SEM, standard error of the mean; SPF, specific pathogen-free; SU, ALV-J envelope glycoprotein; TEAB, triethylamine borane; TMT, tandem mass tag; UPLC, ultra-performance liquid chromatography

* Corresponding author.
E-mail addresses: park_pang@163.com (Y. Pang), zhoudefang@126.com (D. Zhou), xuejingwen19941213@163.com (J. Xue), tiramisurd@163.com (J. Zhou), m17661212469@163.com (Y. Zhang), zgyazad@163.com (G. Zheng), shiyuyuan@163.com (S. Yuan), yongxiu.yao@pirbright.ac.uk (Y. Yao), czqsd@126.com (Z. Cheng).

https://doi.org/10.1016/j.virusres.2019.02.014
Received 8 January 2019; Received in revised form 20 February 2019; Accepted 20 February 2019
Available online 21 February 2019

neointimal smooth muscle cells and adventitial fibroblasts of balloon-injured vessels (Chen et al., 2013; Pyagay et al., 2005). Previous studies showed that CTHRC1 levels are elevated in human solid cancers (Kharaishvili et al., 2011; Tang et al., 2006), such as lung (Ke et al., 2014), breast (Allinen et al., 2004), liver (Chen et al., 2013), ovarian (Hou et al., 2015), and pancreatic (Park et al., 2013) cancer. Additionally, CTHRC1 can facilitate the migration and invasion of tumor cells by activating the Wnt/planar cell-polarity pathway (Ip et al., 2011; Liu et al., 2013; Tano et al., 2010; Wu et al., 2017). Moreover, previous studies identified CTHRC1 to function in the restraint of collagen synthesis (Bian et al., 2015; Shekhani et al., 2016; Wang et al., 2012), which enhances host-cell permeabilization (Jin et al., 2016; Martinez-Gil et al., 2011). Despite having multiple cellular functions, a role for CTHRC1 in retroviral replication has not yet been reported.

In this study, we used a tandem mass-tag (TMT) approach to screen for key differentially expressed cellular proteins associated with ALV-J replication. Based on bioinformatics analysis and experimental data, our results indicated a likely role for CTHRC1 in ALV-J replication according to elevated CTHRC1 levels *in vivo* and *in vitro* upon infection. Importantly, ALV-J-mediated upregulation of CTHRC1 facilitated viral replication through interactions between the ALV-J envelope glycoprotein (SU) and CTHRC1 and CTHRC1 translocation from the nucleus to the cytosol. These results suggest that CTHRC1 acts as a shuttling protein in host cells and through its recruitment into the cytoplasm by ALV-J, promotes viral replication.

2. Materials and methods

2.1. Cells, virus, and animals

DF-1 is a continuous chicken embryonic fibroblast cell line that exhibits normal fibroblastic morphology and is free of endogenous sequences related to leukosis viruses and avian sarcoma. Importantly, DF-1 cells are capable of sustaining ALV-J replication (Himly et al., 1998). DF-1 cells were obtained from ProCell (ProCell, Beijing, China) and cultured in Dulbecco's modified Eagle medium (DMEM) supplemented with 10% fetal calf serum (Biological Industries, Beit HaEmek, Israel), 100 IU mL^{-1} penicillin, and 100 μg mL^{-1} streptomycin sulfate (Solarbio, Beijing, China). Cells were maintained at 37 °C in a 5% CO_2 incubator and infected with 100 μL DMEM containing a 10^4 50% tissue-culture infective dose of ALV-J strain NX0101. Additionally, embryos of specific pathogen-free (SPF) chickens were infected with ALV-J at six embryonic ages and maintained under SPF conditions, after which chickens were then killed at 15-, 22-, and 35-days post-infection. Animal experiments were performed in accordance with the guidelines of the Shandong Agricultural University Animal Care and Use Committee (permit No. SDAU 18-096; July 6, 2018).

2.2. Proteomics analysis

Uninfected DF-1 cells ($n = 3$) and infected with ALV-J DF-1 cells ($n = 3$) were used to extract proteins for analysis. Cells were incubated with a lysis buffer and sonicated on ice (Scientz-IID; Ningbo Scientz Biotechnology Co., Ltd., Ningbo, China), followed by the removal of cell debris by centrifugation. Protein concentrations were measured in the cell supernatant using a bicinchoninic acid assay kit (Qiagen, Hilden, Germany) according to manufacturer instructions. For digestion, the protein solutions were incubated with 5 mM dithiothreitol, alkylated with 10 mM iodoacetamide and diluted by adding 11 mM triethylamine borane (TEAB; Thermo Fisher Scientific, Waltham, MA, USA) concentration to obtain a urea concentration of < 3 M. Trypsin was added at a 1:100 mass ratio (trypsin:protein) to produce peptides, which were desalted using a Strata X C18 SPE column (Phenomenex, Torrance, CA, USA), followed by vacuum drying. Desalted peptides were combined in 0.5 M TEAB and processed using a TMT kit (Thermo Fisher Scientific) according to manufacturer instructions. The tryptic peptides were fractionated using high-pH reversed-phase high-performance liquid chromatography on an Agilent 300Extend C18 column (5-μm particles, 4.6-mm i.d., 250 mm length; Agilent Technologies, Santa Clara, CA, USA) with 0.1% formic acid. The peptide fraction was directly loaded onto an in-house reversed-phase analytical column (15 cm × 75 μm i.d.), and a constant flow was achieved using an EASY-nLC 1000 ultra-performance liquid chromatography (UPLC) system (Thermo Fisher Scientific). The peptides were then subjected to a nanospray ionization source, followed by tandem mass spectrometry (MS/MS) using a Q Exactive Plus mass spectrometer (Thermo Fisher Scientific) coupled online with the UPLC system. The resulting MS/MS data were processed using the MaxQuant search engine (v.1.5.2.8; https://maxquant.org/) and compared with those available in the Uniprot *Gallus gallus* database (https://www.uniprot.org/proteomes/UP000000539) concatenated with a reverse decoy database. To identify differentially expressed proteins, Bonferroni *p*-value adjustments ($p < 10^{-16}$) and paired *t*-tests were performed. Only proteins with a corrected $p < 0.05$ and a fold change > 1.3 were considered differentially expressed. Hierarchical clustering analysis was conducted to produce a visual representation of the expression profiles using TBtools software (https://omictools.com/tbtools-tool). Gene Ontology (GO) annotation was performed to determine the categories of differentially expressed proteins. DAVID software (v.6.8; https://david.ncifcrf.gov/) was employed to determine enriched protein categories, and a two-tailed Fisher's exact test was applied to test the enrichment. Only GO categories with a Fisher's exact test $p < 0.05$ were deemed significantly enriched.

2.3. Reverse transcription and quantitative real-time polymerase chain reaction (qPCR)

Total RNA was extracted from cells and tissues according to manufacturer instructions (Qiagen), and RNA concentration was measured using a spectrophotometer (Qiagen). We used 1 μg of total RNA as a template to synthesize cDNA using a reverse transcriptase kit (TaKaRa, Shiga Japan) according to manufacturer instructions. A SYBR Green I kit (TaKaRa) was used for cDNA amplification in a total volume of 20 μL. *CTHRC1*-specific primers were as follows: forward, 5′-ACGCTG GCTTGGTGGA-3′ and reverse, 5′-CAGTTCTTCAATGATGATACGG-3′. ALV-J-specific primers were as follows: forward, 5′-TGCGTGCGTGGT TATTATTTC-3′ and reverse, 5′-AATGGTGAGGTCGCTGACTGT-3′. Primers for glyceraldehyde 3-phosphate dehydrogenase (*GAPDH*), a housekeeping gene, were as follows: forward, 5′-GAACATCATCCCAG CGTCCA-3′ and reverse, 5′-CGGCAGGTCAGGTCAACAAC-3′. A LightCycler 96 system (Roche, Basel, Switzerland) was used for qPCR with the following cycling conditions: denaturation at 95 °C for 30 s, followed by 40 cycles at 95 °C for 5 s and 60 °C for 34 s A melting curve was generated at 95 °C for 10 s, 65 °C for 60 s, and 97 °C for 1 s. *CTHRC1* levels were analyzed using the $2^{-\Delta\Delta Ct}$ method, and ALV-J load was measured according to an absolute quantification equation: $y = -3.2526x + 39.148$.

2.4. CTHRC1 overexpression and RNA interference (RNAi)

A *CTHRC1*-expression plasmid (pcDNA3.1-CTHRC1) was constructed based on the pcDNA3.1 vector (GenePharma, Shangjai, China). The pGPU6/GFP/Neo plasmid (GenePharma) was used for *CTHRC1* RNAi, and RNA duplexes and control short-hairpin RNA (shRNA; shNC) were synthesized by GenePharma. Target shRNA sequences for *CTHRC1* were as follows: 5′-GCACTGAACTACGGCATAGAC-3′ (1) and 5′-GTCT GTGTGAAGGGATCAACG-3′ (2). At 70% confluence, DF-1 cells were transfected with pcDNA3.1-CTHRC1, shCTHRC1-1, shCTHRC1-2, and shNC (160 nM) using X-tremeGENE HP DNA transfection reagent (Roche) according to manufacturer instructions. After incubation for 8 h and infection with ALV-J for 72 h, the cells were extracted or lysed to detect *CTHRC1* expression and determine the ALV-J load by qPCR and western blot, respectively. Cell supernatant was collected for

enzyme-linked immunosorbent assay (ELISA) experiments.

2.5. Western blot

To evaluate CTHRC1 levels, uninfected and ALV-J-infected DF-1 cells were lysed at 4 °C using radioimmunoprecipitation assay (RIPA) buffer containing phenylmethylsulfonyl fluoride (PMSF; 100:1). Proteins were separated by 15% sodium dodecyl sulfate polyacrylamide gel electrophoresis and transferred onto 0.22-μm polyvinylidene difluoride membranes, which were blocked in 5% Difco skim milk (Solarbio) at 37 °C for 2 h, followed by incubation with primary antibodies diluted with Tris-buffered saline containing Tween-20 at 4 °C overnight. The primary antibodies included rabbit polyclonal anti-CTHRC1 (Absin, Beijing, China) and anti-β-actin (Thermo Fisher Scientific) and an in-house mouse monoclonal anti-ALV-J gp85 antibody (1D4). Following overnight incubation, species-specific secondary (Abbkin, Beijing, China) antibodies were applied at 37 °C for 1 h, and the membranes were exposed to an X-ray film.

2.6. Immunohistochemistry

To determine CTHRC1 localization in tissues and cells, immunohistochemical staining was performed on formalin-fixed, paraffin-embedded, and sectioned (4-μm thick) sections using a rotary microtome (Leica, Wetzlar, Germany). Slides were treated with a sodium citrate solution (pH 6.0) by microwaving four times for 5 min each to retrieve antigens. The slides were cooled at room temperature and blocked using H_2O_2 for 1 h at 37 °C, followed by incubation with the anti-CTHRC1 antibody (1:400) overnight at 4 °C and washing three times with phosphate-buffered saline (PBS). The slides were then incubated with biotinylated goat anti-rabbit IgG for 45 min at 37 °C and washed with PBS three times. An enhanced horseradish peroxidase-3,3′-diaminobenzidine chromogenic substrate (Qiagen) was applied to the slides for 35 s to visualize the staining reaction, followed by washing with PBS. The slides were counterstained with Mayer's hematoxylin for 6 min, dehydrated in a graded series of alcohol, and sealed with coverslips. Images were visualized and captured under a light microscope (Olympus BX53).

2.7. Confocal laser scanning microscopy (CLSM) assay

DF-1 cells were seeded on sterile coverslips, infected with ALV-J at 70% confluence, and maintained for 72 h with DMEM containing 1% bovine serum albumin at 37 °C in a 5% CO_2 incubator. The cells were fixed with an ice-cold mixture of acetone and ethanol (3:2) for 9 min, washed three times with PBS, and blocked with PBS containing 10% neonatal calf serum for 1 h at room temperature. The cells were then incubated with the anti-CTHRC1 and anti-ALV-J primary antibodies for 12 h at 4 °C, followed by incubation with fluorescein isothiocyanate (FITC)-labeled goat anti-rabbit (for CTHRC1) or Alexa Fluor 647-labeled goat anti-rabbit (for ALV-J) secondary antibodies for 50 min. After staining cell nuclei with 4′,6-diamidino-2-phenylindole (DAPI), the slides were covered with 50% glycerol and observed by CLSM (Leica SP8).

2.8. Co-immunoprecipitation assay (Co-IP)

DF-1 cells were seeded in a 25-cm^2 tissue-culture flask, grown to 70% confluence, infected with ALV-J, harvested at 72-h post-infection, and lysed on ice for 15 min in RIPA buffer containing PMSF (100:1). The lysates were clarified by centrifugation at 17,000*g* for 10 min at 4 °C and then incubated with the ALV-J gp85 monoclonal antibody (1D4) for up to 20 min at room temperature. A Co-IP assay was performed using the Capturem IP & Co-IP kit (TaKaRa) according to manufacturer instructions. Western blot was performed to analyze the samples. To detect immunoprecipitated CTHRC1 and ALV-J SU, the VeriBlot secondary antibody (Abcam, Cambridge, UK) was used.

2.9. ELISA

ELISA kits were used to measure CTHRC1 (Sanbeiji, Nanjing, China) and p27 (IDEXX Laboratories, Westbrook, ME, USA) levels in cell supernatant according to manufacturer instructions. Each experiment included three biological replicates.

2.10. Statistical analysis

All data are reported as the mean ± standard error of the mean (SEM). Prism 7.0 software (GraphPad Software, San Diego, CA, USA) was used to determine statistically significant differences by performing a two-tailed unpaired Student's *t*-test. A $p < 0.05$ was considered statistically significant.

3. Results

3.1. CTHRC1 levels are significantly upregulated in ALV-J-infected cells

ALV-J replication depends strongly upon the host cell cycle (Scholle et al., 2004) and the virus supports its lifecycle by interfering with host cell processes and exploiting host proteins. To identify the cellular proteins required for ALV-J replication, we performed a TMT-based proteomics analysis and used hierarchical clustering to visualize changes in the abundance of differentially expressed proteins between groups (Fig. 1A). We identified 88 differentially expressed proteins (fold change > 1.3), of which 40 (45%) were upregulated and 48 (55%) were downregulated in ALV-J-infected cells relative to their expression in uninfected cells. As shown in Fig. 1B, the $-\log(P)$ value of each protein was plotted against the $\log_2$ ratio of the intensity observed in ALV-J-infected cells and relative to controls, revealing similar patterns of regulation, although a higher number of downregulated proteins according to *p*-values. GO functional analysis indicated that the differentially expressed proteins were predominantly associated with the extracellular space (Cell Component), protein-glutamine gamma-glutamyltransferase activity (Molecular Function), and peptide cross-linking (Biological Process) (Fig. 1C). Proteomics analysis revealed an ALV-J-related fold-change in CTHRC1 levels of > 1.5 and significant enrichment in the extracellular region. These results suggested the potential involvement of CTHRC1 in ALV-J replication.

3.2. ALV-J facilitates CTHRC1 expression in vitro and in vivo

Evaluation of CTHRC1 mRNA and proteins in ALV-J-infected and uninfected DF-1 cells showed that *CTHRC1* mRNA levels were significantly upregulated in infected cells relative to uninfected cells (Fig. 2A). Similarly, we observed time-dependent elevations in CTHRC1 protein levels in ALV-J-infected cells post-infection (Fig. 2B and C). Additionally, we observed similar time-dependent increases in the ALV-J load assessed by qPCR and p27 levels post-infection (Fig. 2D and E). These results suggested that ALV-J infection upregulated CTHRC1 levels *in vitro*.

We then investigated CTHRC1 effects on ALV-J replication *in vivo* by establishing a congenital ALV-J infection model using 6-day-old embryos. After hatching, the chicks were killed at 1, 7, and 20 days of age for immunohistochemistry assays. The results showed that both the number of CTHRC1-positive cells and CTHRC1 levels were substantially higher in ALV-J-infected chickens than in uninfected chickens (Fig. 2F). Moreover, the CTHRC1-positive signal was predominantly localized to the cytosol in ALV-J-infected tissues. These results showed that ALV-J infection increases in CTHRC1 levels *in vitro* and *in vivo*.

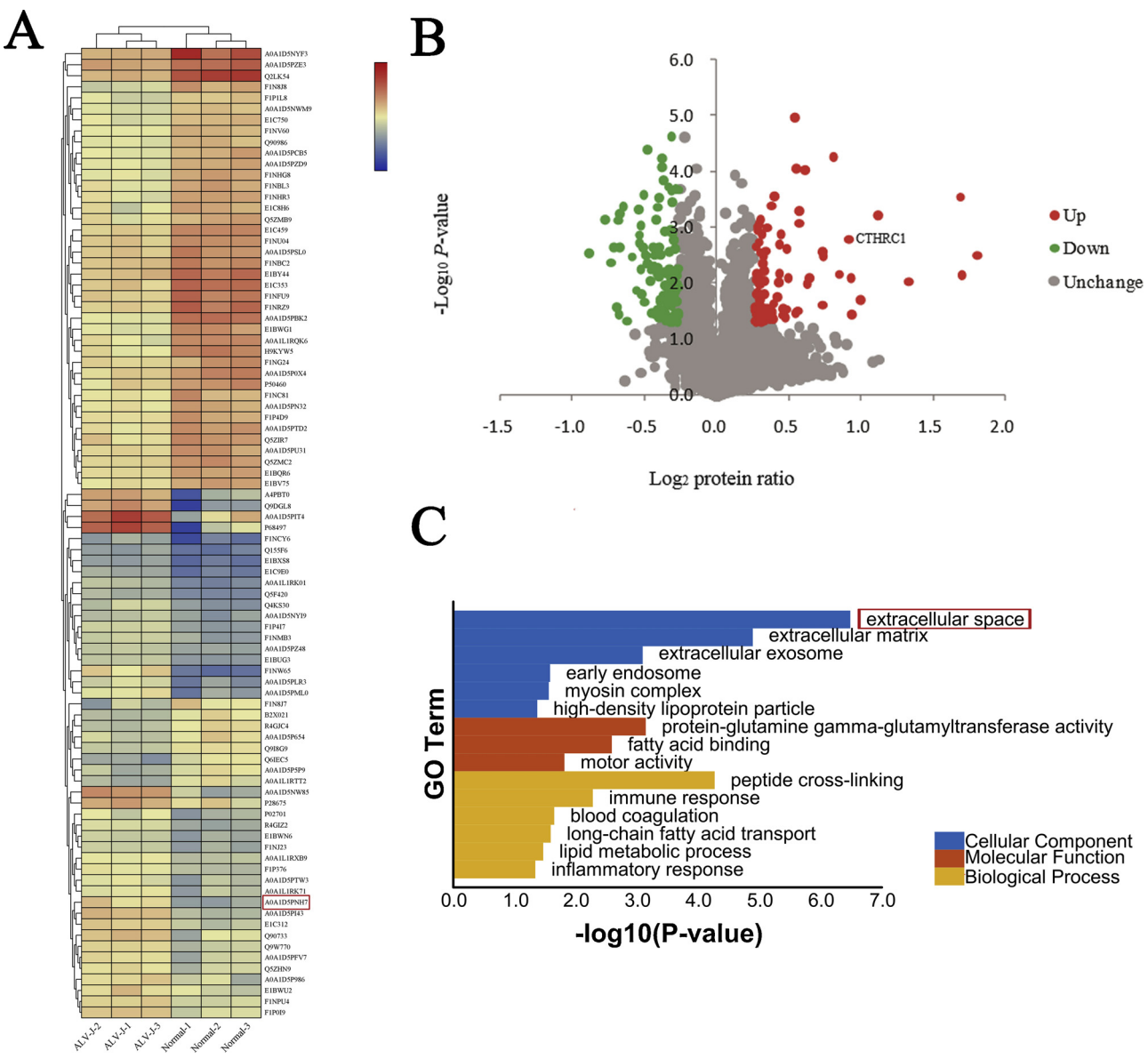

Fig. 1. CTHRC1 levels are significantly upregulated in ALV-J-infected cells. (A) Clustering of 88 proteins displaying significant differential levels between infected and uninfected cells. Input data were the $\log_2$ ratios of the intensity in ALV-J-infected cells to that in uninfected cells. Red color indicates upregulated proteins, and blue color indicates downregulated proteins. (B) Volcano plot of all proteins. The $-\log$ (P) of each protein is plotted against the $\log_2$ ratio of the intensity in ALV-J-infected cells to that in uninfected cells. Red dots indicate upregulated proteins in ALV-J infected cells, and blue dots indicated downregulated proteins. (C) GO functional analysis. Blue color represents Cell Composition, orange color represents Molecular Function, and yellow color represents Biological Processes. The red box indicates the location of CTHRC1.

3.3. *CTHRC1 overexpression promotes ALV-J replication*

To determine whether elevated levels of CTHRC1 are associated with increased ALV-J load, we transfected a recombinant pcDNA3.1-CTHRC1 plasmid into DF-1 cells, followed by confirmation by qPCR, western blot, and ELISA of elevated CTHRC1 mRNA and protein levels (Fig. 3A–C). Additionally, we found increased levels of CTHRC1 also increased levels of intracellular ALV-J RNA and viral proteins, as well as extracellular ALV-J protein (Fig. 3C–E). These data suggested that *CTHRC1* overexpression promoted ALV-J replication.

3.4. *CTHRC1 knockdown decreases ALV-J replication*

Because *CTHRC1* overexpression facilitated ALV-J replication, we hypothesized that *CTHRC1* knockdown might negatively affect ALV-J replication. To test this hypothesis, we transiently transfected DF-1 cells with shRNA targeting *CTHRC1* and harvested the cells at 72-h post-infection with ALV-J. We verified that *CTHRC1* expression was downregulated following shRNA transfection (Fig. 4A), and confirmed that CTHRC1 levels were also downregulated by ˜35% relative to levels in control DF-1 cells (Fig. 4B–D). Moreover, we found that downregulation of CTHRC1 levels significantly reduced ALV-J replication in *CTHRC1*-silenced DF-1 cells (Fig. 4D–F). These results suggested that CTHRC1 is involved in ALV-J replication.

3.5. *CTHRC1 interacts with the ALV-J SU protein in the cytoplasm*

To investigate interactions between CTHRC1 and ALV-J and whether CTHRC1 localization changes following ALV-J infection, we performed CLSM and Co-IP analyses. The results showed that CTHRC1 localized to the nucleus in normal cells, whereas it localized to the cytoplasm in ALV-J-infected cells. These findings suggested a role for

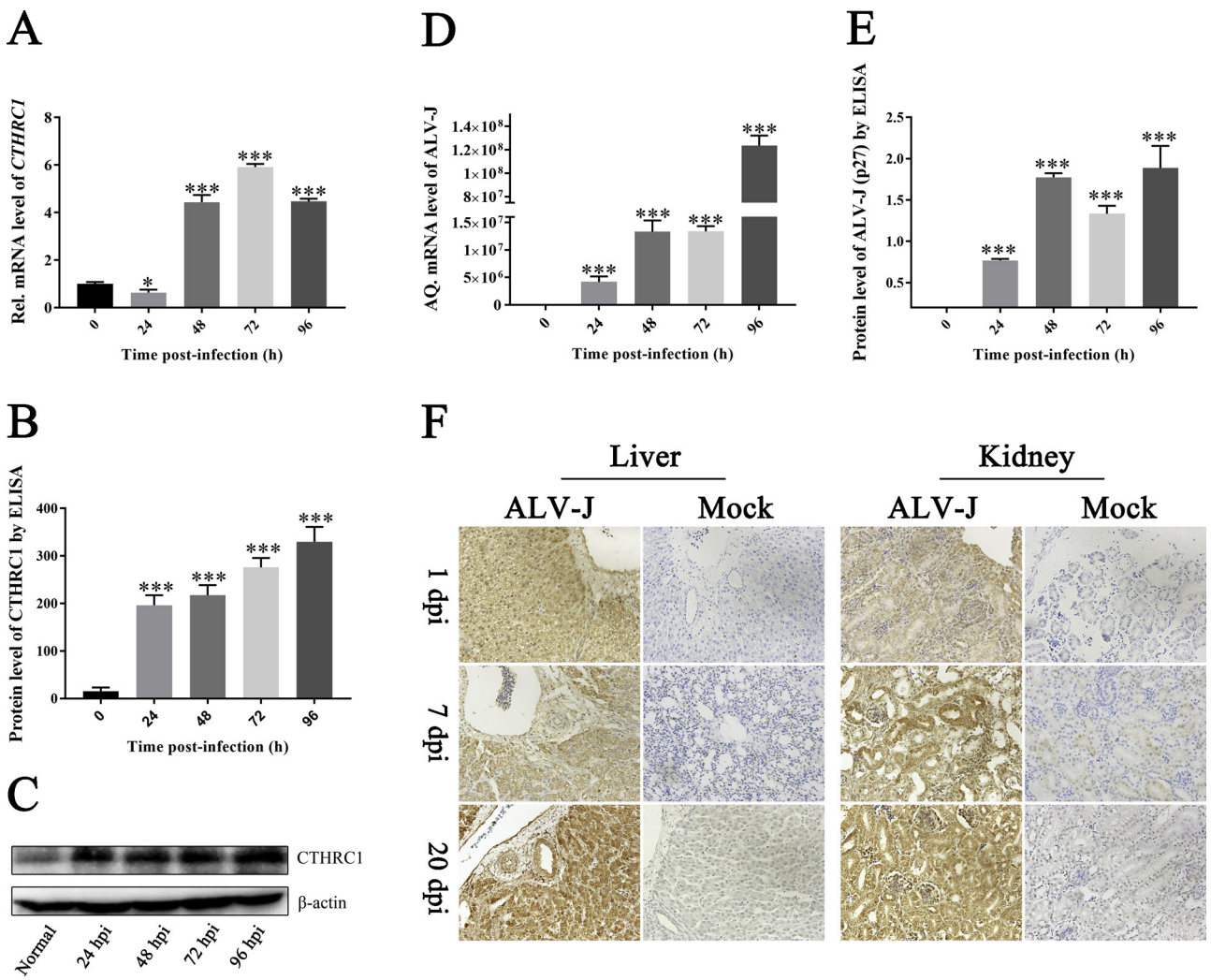

Fig. 2. ALV-J infection facilitates *CTHRC1* expression *in vitro* and *in vivo*. (A and D) Total RNA was extracted from ALV-J-infected and uninfected DF-1 cells. *CTHRC1* mRNA and ALV-J copy number were measured by qPCR. (B and E) CTHRC1 and ALV-J p27 proteins were measured by ELISA in supernatant from ALV-J-infected and uninfected DF-1 cells. (C) CTHRC1 protein levels detected by western blot in ALV-J-infected and uninfected DF-1 cells. (F) CTHRC1 protein levels measured by immunohistochemistry. Data are presented as mean ± SEM ($n = 3$). $^{*}p < 0.05$; $^{***}p < 0.001$. dpi, days post-infection.

CTHRC1 as a shuttle protein, and that ALV-J induces CTHRC1 translocation from the nucleus to the cytoplasm.

CLSM results confirmed ALV-J-mediated upregulation of CTHRC1 levels, suggesting inducible activation of CTHRC1 and its role in promoting ALV-J replication. Moreover, the merged fluorescence images of ALV-J and CTHRC1 indicated interactions between the ALV-J SU protein and CTHRC1 and revealed that the interaction occurred in the cytoplasm (Fig. 5A). Furthermore, Co-IP results confirmed the interaction between the ALV-J SU protein and CTHRC1 (Fig. 5B).

4. Discussion

The ALV-J lifecycle is highly dependent upon cellular proteins. Identification of host proteins involved in ALV-J replication not only increases the understanding of the ALV-J lifecycle but also aids in the development of novel anti-ALV-J therapies. Because mutation rates in cellular proteins are substantially lower than those in viral genomes, targeting host proteins might represent an effective barrier to the generation of drug resistance. To identify the cellular proteins involved in ALV-J replication, we used proteomics analysis to screen key host proteins associated with viral replication. We identified CTHRC1, a multifunctional protein that plays an important role in human solid tumors through various signaling pathways (Chen et al., 2017; Liu et al., 2013). Previous investigations of CTHRC1 focused on the invasion and migration of human solid tumors (Chen et al., 2013; Liu et al., 2018; Wang et al., 2017; Ye et al., 2016); however, there are few studies addressing the effect of CTHRC1 on viral replication. One such study indicated that CTHRC1 supports hepatitis B virus (HBV) replication in cultured cells and Balb/c mice by activating the protein kinase α/extracellular-signal-regulated kinase/Janus N-terminal kinase/c-Jun cascade to inhibit the interferon-mediated Janus kinase/signal transducer of activation signaling pathway (Bai et al., 2015). In the present study, we showed that *CTHRC1* knockdown significantly reduced extracellular ALV-J protein levels, as well as intracellular ALV-J RNA and protein levels, suggesting that CTHRC1 is required for ALV-J replication.

To screen proteins associated with ALV-J replication, we used a TMT method, followed by bioinformatics analysis. Our results revealed substantial upregulation of CTHRC1 levels (fold-change > 1.5) in ALV-J-infected cells, and GO functional analysis revealed enrichment of the protein in the extracellular space. Previous studies reported that *CTHRC1* overexpression inhibits collagen type I and III deposition (Pyagay et al., 2005; Shekhani et al., 2016), which can alter host cell-membrane permeabilization to promote viral replication (Martinez-Gil et al., 2011). Based on these findings and our data, we suggest that CTHRC1 might be associated with ALV-J replication.

CTHRC1 has characteristics similar to those of circulating hormones

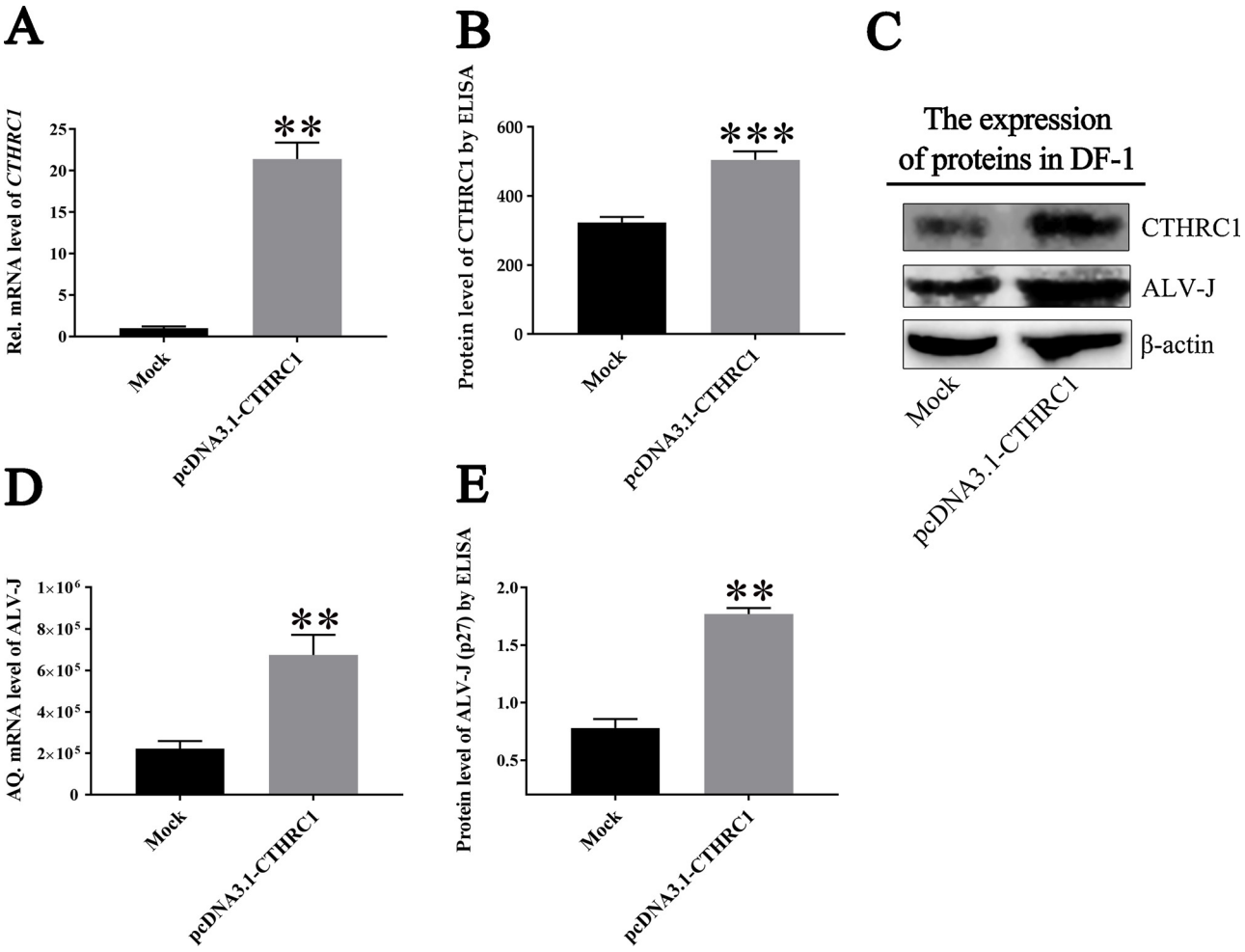

Fig. 3. *CTHRC1* overexpression facilitates ALV-J replication. (A and D) Total RNA was extracted from DF-1 cells transfected with the pcDNA3.1-CTHRC1 or a control plasmid (pcDNA3.1), followed by infection with ALV-J. *CTHRC1* mRNA and ALV-J load were measured by qPCR. (B and E) Supernatant from cells transfected with pcDNA3.1-CTHRC1 or pcDNA3.1 and infected with ALV-J and subjected to ELISA for CTHRC1 and p27. (C) CTHRC1 and ALV-J SU protein levels detected by western blot in DF-1 cells transfected with pcDNA3.1-CTHRC1 or pcDNA3.1 and infected with ALV-J. Data are presented as mean ± SEM ($n = 3$). $^{**}p < 0.01$; $^{***}p < 0.001$. AQ, ALV-J absolute fluorescence quantification.

by exhibiting a wide range of effects on cellular physiology and metabolism (Stohn et al., 2012). To investigate the CTHRC1 function during viral replication, we demonstrated that CTHRC1 facilitated ALV-J replication in cultured cells and an animal model, finding that upregulated CTHCR1 levels promoted ALV-J replication, and that *CTHRC1* knockdown significantly attenuated ALV-J replication. These data suggested that ALV-J activated *CTHRC1* expression *in vitro* and *in vivo*, and that the virus required the host protein to enable self-replication.

Interactions between host proteins and viral factors within subcellular compartments are required for viral genome replication (Bender et al., 2014; Penfold and Mocarski, 1997). In the present study, we used CLSM and Co-IP to investigate changes in CTHRC1 localization and possible interactions between CTHRC1 and ALV-J, respectively. The results demonstrated that CTHRC1 was predominantly and diffusely distributed throughout the nucleus, with very low cytoplasmic expression observed in uninfected cells. However, during ALV-J infection, CTHRC1 localization changed from the nucleus to the cytoplasm. Moreover, Co-IP results indicated that the ALV-J SU protein interacts with CTHRC1, suggesting a role for SU in promoting CTHRC1 recruitment and translocation.

5. Conclusion

In summary, we showed that ALV-J infection induces *CTHRC1* expression both *in vivo* and *in vitro*, and that ALV-J-mediated upregulation of CTHRC1 levels facilitated viral replication through interactions between the ALV-J SU protein and CTHRC1. These results suggest that CTHRC1 is a host-cell protein that is hijacked by ALV-J to promote viral replication and provide novel insights into the regulatory mechanisms associated with ALV-J infection. Although the molecular mechanisms by which CTHRC1 enhances ALV-J replication require further investigation, our findings propose CTHRC1 as a potential target for antiviral-drug development.

Funding information

The study was supported by grants from the China-UK Partnership on Global Food Security: Combating avian tumor diseases for sustainable poultry production (31761133002, BB/R012865/1), the Natural Science Foundation of China (31672521), the Shandong Modern Agricultural Technology & Industry System (SDAIT-11-04) and the Fund of Shandong “Double Tops” Program (2017).

Authors and contributors

Ziqiang Cheng and Yu Pang conceived and designed the experiments; Yu Pang performed the experiments; Yu Pang, Defang Zhou, Jingwen Xu, Jing Zhou, Ya Zhang, Gaoying Zheng and Shiyu Yuan

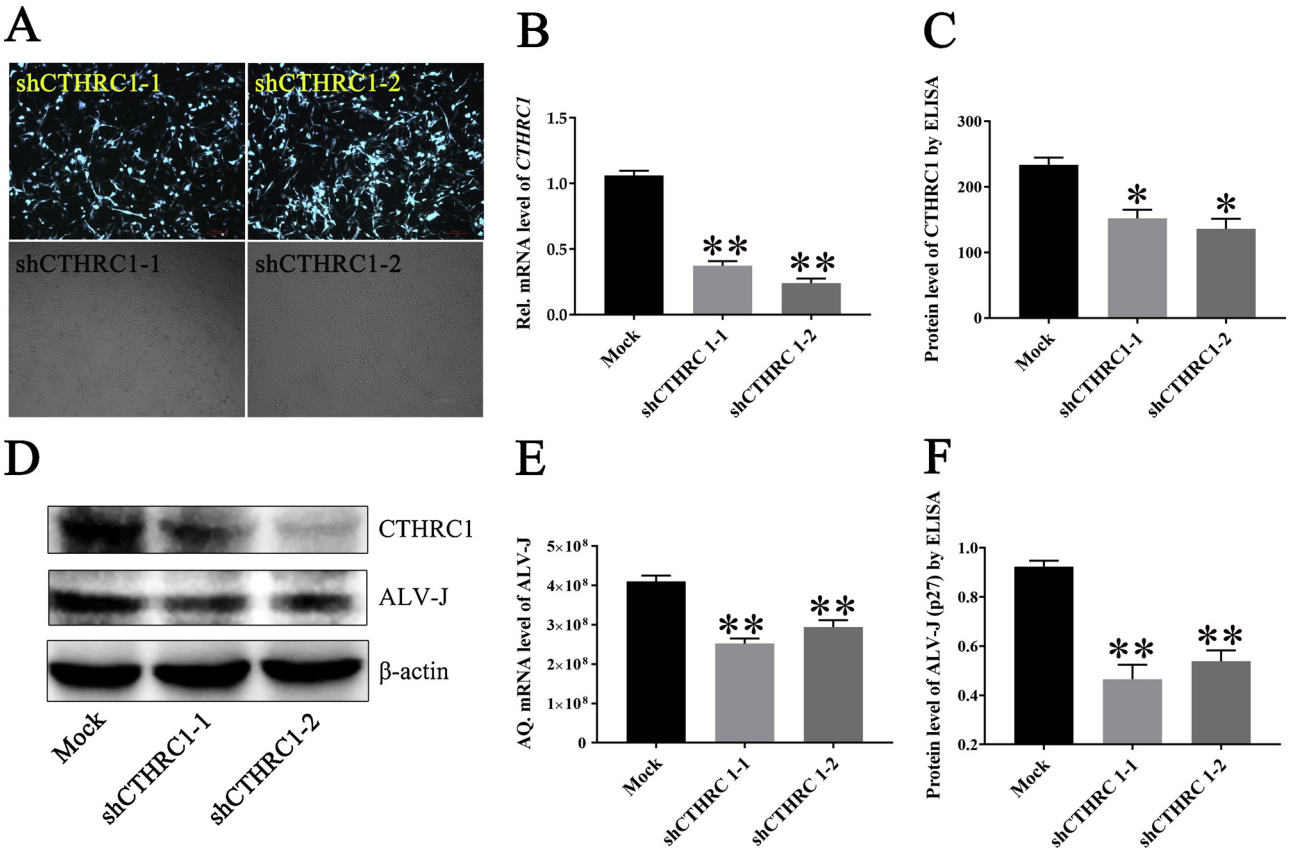

Fig. 4. *CTHRC1* knockdown decreases ALV-J replication. (A) Following transfection of DF-1 cells with shCTHRC1-1 and shCTHRC1-2, fluorescence was observed by inverted fluorescence microscopy. (B and E) Total RNA was extracted from DF-1 cells transfected with shRNAs (shCTHRC1-1, shCTHRC1-2, or shNC) and infected with ALV-J. *CTHRC1* mRNA and ALV-J viral load were measured by qPCR. (C and F) Supernatant from cells transfected with shRNAs (shCTHRC1-1, shCTHRC1-2, or shNC) and infected with ALV-J were subjected to ELISA for CTHRC1 and p27. (D) CTHRC1 and ALV-J gp85 protein levels detected by western blot in DF-1 cells transfected with shRNAs (shCTHRC1-1, shCTHRC1-2, or shNC) and infected with ALV-J. Data represent the mean ± SEM ($n = 3$). *$p < 0.05$; **$p < 0.01$.

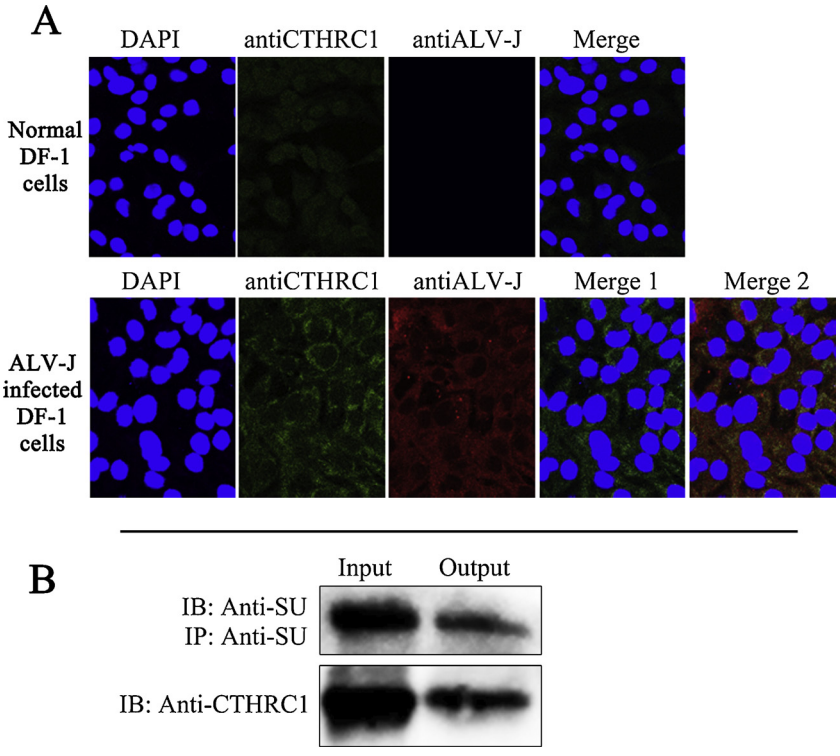

Fig. 5. CTHRC1 directly interacts with the ALV-J SU protein and translocates to the cytosol following ALV-J infection. (A) CTHRC1 was stained using an anti-CTHRC1 antibody and FITC. The SU protein of ALV-J was detected using an anti-gp85 antibody and Alexa Fluor 647. Nuclei were visualized using DAPI. Merge 1 indicates the combination of nuclear and anti-ALV-J staining, and Merge 2 indicates the combination of nuclear, anti-ALV-J, and anti-CTHRC1 staining. (B) DF-1 cells were collected at 72-h post-infection with ALV-J. Lysates were immunoprecipitated with the anti-gp85 antibody and detected by western blot using the anti-CTHRC1 antibody.

analyzed the data; Yongxiu Yao revised the manuscript; Ziqiang Cheng and Yu Pang wrote the paper.

Ethical approval

The animal experiments were agreed by the Shandong Animal Care and Use Committee (permit number: SDAU number 18-096, 6 July 2018).

Acknowledgements

We are grateful to the Teacher, Li Zhang for providing the necessary infrastructure facilities for the study.

Conflicts of Interest

The authors declare no conflict of interest.

References

Allinen, M., Beroukhim, R., Cai, L., Brennan, C., Lahti-Domenici, J., Huang, H., Porter, D., Hu, M., Chin, L., Richardson, A., Schnitt, S., Sellers, W.R., Polyak, K., 2004. Molecular characterization of the tumor microenvironment in breast cancer. Cancer Cell 6 (1), 17–32.

Bai, L., Zhang, W., Tan, L., Yang, H., Ge, M., Zhu, C., Zhang, R., Cao, Y., Chen, J., Luo, Z., Ho, W., Liu, F., Wu, K., Wu, J., 2015. Hepatitis B virus hijacks CTHRC1 to evade host immunity and maintain replication. J. Mol. Cell Biol. 7 (6), 543–556.

Bender, B.J., Coen, D.M., Strang, B.L., 2014. Dynamic and nucleolin-dependent localization of human cytomegalovirus UL84 to the periphery of viral replication compartments and nucleoli. J. Virol. 88 (20), 11738–11747.

Bian, Z., Miao, Q., Zhong, W., Zhang, H., Wang, Q., Peng, Y., Chen, X., Guo, C., Shen, L., Yang, F., Xu, J., Qiu, D., Fang, J., Friedman, S., Tang, R., Gershwin, M.E., Ma, X., 2015. Treatment of cholestatic fibrosis by altering gene expression of Cthrc1: Implications for autoimmune and non-autoimmune liver disease. J. Autoimmun. 63, 76–87.

Chen, Y.L., Wang, T.H., Hsu, H.C., Yuan, R.H., Jeng, Y.M., 2013. Overexpression of CTHRC1 in hepatocellular carcinoma promotes tumor invasion and predicts poor prognosis. PLoS One 8 (7), e70324.

Chen, G., Wang, D., Zhao, X., Cao, J., Zhao, Y., Wang, F., Bai, J., Luo, D., Li, L., 2017. miR-155-5p modulates malignant behaviors of hepatocellular carcinoma by directly targeting CTHRC1 and indirectly regulating GSK-3beta-involved Wnt/beta-catenin signaling. Cancer Cell Int. 17, 118.

Cheng, Z.Q., Zhang, L., Liu, S.D., Zhang, L.J., Cui, Z.Z., 2005. Emerging of avian leukosis virus subgroup J in a flock of Chinese local breed. Wei Sheng Wu Xue Bao 45 (4), 584–587.

Feng, M., Tan, Y., Dai, M., Li, Y., Xie, T., Li, H., Shi, M., Zhang, X., 2016. Endogenous retrovirus ev21 dose not recombine with ALV-J and induces the expression of ISGs in the host. Front. Cell. Infect. Microbiol. 6, 140.

Himly, M., Foster, D.N., Bottoli, I., Iacovoni, J.S., Vogt, P.K., 1998. The DF-1 chicken fibroblast cell line: transformation induced by diverse oncogenes and cell death resulting from infection by avian leukosis viruses. Virology 248 (2), 295–304.

Hou, M., Cheng, Z., Shen, H., He, S., Li, Y., Pan, Y., Feng, C., Chen, X., Zhang, Y., Lin, M., 2015. High expression of CTHRC1 promotes EMT of epithelial ovarian cancer (EOC) and is associated with poor prognosis. Oncotarget 6 (34), 35813–35829.

Ip, W., Wellman-Labadie, O., Tang, L., Su, M., Yu, R., Dutz, J., Wang, Y., Huang, S., Zhang, X., Huang, C., 2011. Collagen triple helix repeat containing 1 promotes melanoma cell adhesion and survival. J. Cutan. Med. Surg. 15 (2), 103–110.

Jin, X.F., Li, H., Zong, S., Li, H.Y., 2016. Knockdown of collagen triple Helix repeat containing-1 inhibits the proliferation and epithelial-to-mesenchymal transition in renal cell carcinoma cells. Oncol. Res. 24 (6), 477–485.

Ke, Z., He, W., Lai, Y., Guo, X., Chen, S., Li, S., Wang, Y., Wang, L., 2014. Overexpression of collagen triple helix repeat containing 1 (CTHRC1) is associated with tumour aggressiveness and poor prognosis in human non-small cell lung cancer. Oncotarget 5 (19), 9410–9424.

Kharaishvili, G., Cizkova, M., Bouchalova, K., Mgebrishvili, G., Kolar, Z., Bouchal, J., 2011. Collagen triple helix repeat containing 1 protein, periostin and versican in primary and metastatic breast cancer: an immunohistochemical study. J. Clin. Pathol. 64 (11), 977–1082.

Lesbats, P., Parissi, V., 2018. Retroviral integration site selection: a running Gag? Microbial Cell (Graz, Austria) 5 (12), 569–571.

Li, Y., Fu, J., Cui, S., Meng, F., Cui, Z., Fan, J., Chang, S., Zhao, P., 2017. Gp85 genetic diversity of avian leukosis virus subgroup J among different individual chickens from a native flock. Poult. Sci. 96 (5), 1100–1107.

Lin, W., Li, X., Dai, Z., Zhang, X., Chang, S., Zhao, P., Zhang, H., Chen, F., Xie, Q., 2016. Molecular epidemiology of J-subgroup avian leukosis virus isolated from meat-type chickens in southern China between 2013 and 2014. Arch. Virol. 161 (11), 3039–3046.

Liu, G., Sengupta, P.K., Jamal, B., Yang, H.Y., Bouchie, M.P., Lindner, V., Varelas, X., Kukuruzinska, M.A., 2013. N-glycosylation induces the CTHRC1 protein and drives oral cancer cell migration. J. Biol. Chem. 288 (28), 20217–20227.

Liu, J., Chen, Z., Xiang, J., Gu, X., 2018. MicroRNA-155 acts as a tumor suppressor in colorectal cancer by targeting CTHRC1 in vitro. Oncol. Lett. 15 (4), 5561–5568.

Ma, M.Z., Zhuang, C., Yang, X.M., Zhang, Z.Z., Ma, H., Zhang, W.M., You, H., Qin, W., Gu, J., Yang, S., Cao, H., Zhang, Z.G., 2014. CTHRC1 acts as a prognostic factor and promotes invasiveness of gastrointestinal stromal tumors by activating Wnt/PCP-Rho signaling. Neoplasia 16 (3), 265–278 278 e261-213.

Martinez-Gil, L., Bano-Polo, M., Redondo, N., Sanchez-Martinez, S., Nieva, J.L., Carrasco, L., Mingarro, I., 2011. Membrane integration of poliovirus 2B viroporin. J. Virol. 85 (21), 11315–11324.

Park, E.H., Kim, S., Jo, J.Y., Kim, S.J., Hwang, Y., Kim, J.M., Song, S.Y., Lee, D.K., Koh, S.S., 2013. Collagen triple helix repeat containing-1 promotes pancreatic cancer progression by regulating migration and adhesion of tumor cells. Carcinogenesis 34 (3), 694–702.

Payne, L.N., Nair, V., 2012. The long view: 40 years of avian leukosis research. Avian Pathol. 41 (1), 11–19.

Payne, L.N., Brown, S.R., Bumstead, N., Howes, K., Frazier, J.A., Thouless, M.E., 1991. A novel subgroup of exogenous avian leukosis virus in chickens. J. Gen. Virol. 72 (Pt 4), 801–807.

Penfold, M.E., Mocarski, E.S., 1997. Formation of cytomegalovirus DNA replication compartments defined by localization of viral proteins and DNA synthesis. Virology 239 (1), 46–61.

Peng, H., Qin, L., Bi, Y., Wang, P., Zou, G., Li, J., Yang, Y., Zhong, X., Wei, P., 2015. Rapid detection of the common avian leukosis virus subgroups by real-time loop-mediated isothermal amplification. Virol. J. 12, 195.

Pyagay, P., Heroult, M., Wang, Q., Lehnert, W., Belden, J., Liaw, L., Friesel, R.E., Lindner, V., 2005. Collagen triple helix repeat containing 1, a novel secreted protein in injured and diseased arteries, inhibits collagen expression and promotes cell migration. Circ. Res. 96 (2), 261–268.

Scholle, F., Li, K., Bodola, F., Ikeda, M., Luxon, B.A., Lemon, S.M., 2004. Virus-host cell interactions during hepatitis C virus RNA replication: impact of polyprotein expression on the cellular transcriptome and cell cycle association with viral RNA synthesis. J. Virol. 78 (3), 1513–1524.

Shekhani, M.T., Forde, T.S., Adilbayeva, A., Ramez, M., Myngbay, A., Bexeitov, Y., Lindner, V., Adarichev, V.A., 2016. Collagen triple helix repeat containing 1 is a new promigratory marker of arthritic pannus. Arthritis Res. Ther. 18 (1), 171.

Smith, L.M., Toye, A.A., Howes, K., Bumstead, N., Payne, L.N., Venugopal, K., 1999. Novel endogenous retroviral sequences in the chicken genome closely related to HPRS-103 (subgroup J) avian leukosis virus. J. Gen. Virol. 80 (Pt 1), 261–268.

Stohn, J.P., Perreault, N.G., Wang, Q., Liaw, L., Lindner, V., 2012. Cthrc1, a novel circulating hormone regulating metabolism. PLoS One 7 (10), e47142.

Sun, S., Cui, Z., 2007. Epidemiological and pathological studies of subgroup J avian leukosis virus infections in Chinese local "yellow" chickens. Avian Pathol. 36 (3), 221–226.

Tang, L., Dai, D.L., Su, M., Martinka, M., Li, G., Zhou, Y., 2006. Aberrant expression of collagen triple helix repeat containing 1 in human solid cancers. Clin. Cancer Res. 12 (12), 3716–3722.

Tano, K., Mizuno, R., Okada, T., Rakwal, R., Shibato, J., Masuo, Y., Ijiri, K., Akimitsu, N., 2010. MALAT-1 enhances cell motility of lung adenocarcinoma cells by influencing the expression of motility-related genes. FEBS Lett. 584 (22), 4575–4580.

Wang, P., Fang, J.Y., 2010. The relationship between CTHRC1 and cancer. Chin. Bull. Life Sci. 22 (8), 797–800.

Wang, P., Wang, Y.C., Chen, X.Y., Shen, Z.Y., Cao, H., Zhang, Y.J., Yu, J., Zhu, J.D., Lu, Y.Y., Fang, J.Y., 2012. CTHRC1 is upregulated by promoter demethylation and transforming growth factor-beta1 and may be associated with metastasis in human gastric cancer. Cancer Sci. 103 (7), 1327–1333.

Wang, C., Li, Z., Shao, F., Yang, X., Feng, X., Shi, S., Gao, Y., He, J., 2017. High expression of Collagen Triple Helix Repeat Containing 1 (CTHRC1) facilitates progression of oesophageal squamous cell carcinoma through MAPK/MEK/ERK/FRA-1 activation. J. Exp. Clin. Cancer Res. 36 (1), 84.

Wang, P., Lin, L., Li, H., Shi, M., Gu, Z., Wei, P., 2018. Full-length genome sequence analysis of an avian leukosis virus subgroup J (ALV-J) as contaminant in live poultry vaccine: The commercial live vaccines might be a potential route for ALV-J transmission. Transbound. Emerg. Dis. 65 (4), 1103–1106.

Wu, Q., Yang, Q., Sun, H., 2017. Role of collagen triple helix repeat containing-1 in tumor and inflammatory diseases. J. Cancer Res. Ther. 13 (4), 621–624.

Ye, J., Chen, W., Wu, Z.Y., Zhang, J.H., Fei, H., Zhang, L.W., Wang, Y.H., Chen, Y.P., Yang, X.M., 2016. Upregulated CTHRC1 promotes human epithelial ovarian cancer invasion through activating EGFR signaling. Oncol. Rep. 36 (6), 3588–3596.